

Characterization of Magnetic Glitches in VSR4 data using correlations between Omicron triggers

Daniel Vander-Hyde¹, Dr. Irene Fiori, Dr. Florent Robinet, Dr. Bas Swinkels

¹California State University, Fullerton, 800 N. State College Blvd., Fullerton, CA 92831-3599

Abstract

A thorough investigation was made into finding the source and coupling mechanisms of magnetic transients at the Virgo site. Approximately five days of data were taken and analyzed from Virgo Science Run #4 (VSR4): from August 2, 14:18:00 2011 to August 7, 14:20:00 2011 (UTC time). This investigation was performed with of MatLab scripts that isolate interesting data from the manipulation of triggers generated by Omicron for various magnetometers, ammeters, and voltmeters.

Introduction

Einstein's theory of general relativity predicts that astrophysical events such as binary black hole inspirals, neutron star mergers, supernovae, etc. produce a disturbance in four-dimensional space-time in the form of gravitational waves (GW). The unit space length change caused by a GW is known as *strain*: $h = \Delta L/L$. Strain values, for relatively nearby astrophysical phenomena, tend to be on the order of 10^{-21} [1]. Existing GW detectors (Virgo, LIGO, GEO, TAMA) aim to measure these tiny warping of space-time through the method of Interferometry based on a Michelson scheme. The adopted scheme consists of a central mirror (BS) splitting the incident laser beam into two perpendicular beams, each resonating through one Fabry-Pérot (FP) optical cavity of length L with suspended mirror test masses at the two ends. The two FP cavities form the "arms" of the interferometer (ITF). The length of the resonant FP cavity is tuned such that, in the absence of GWs, the two beams returning back to the BS destructively interfere and, ideally, the photo detector placed at the ITF output port measures no light. A GW causes a differential length change of the two arms and consequently a phase shift of the two returning beams out of the BS, which is revealed by the photodiode as an increase of light power. Figure 1 shows the optical layout of Virgo, a gravitational wave detector with 3km long arms,

located near Cascina (Italy).

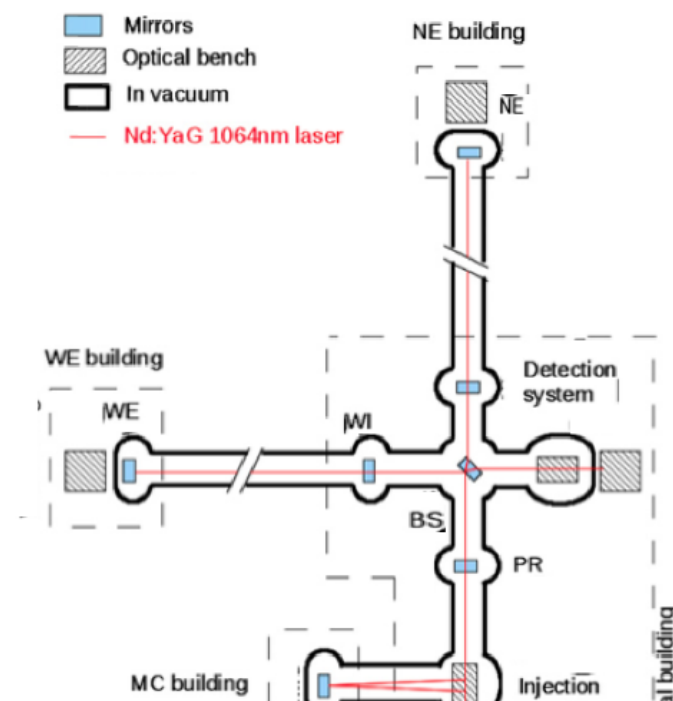


(Figure 1) A schematic of the VIRGO interferometer. The two arms (North arm and West arm) are defined by their general direction with respect to the central Building. The Mode Cleaner (MC), West End (WE), and North End (NE) buildings are labeled accordingly.

Although extreme precautions have been taken to isolate the detector from the external environment (i.e. test mass mirrors are kept in ultra-high vacuum and are mechanically isolated from the ground with the use of Super Attenuators [2]) external disturbances can “couple” to the detector and mimic the effect of a GW thus producing false GW events. Both continuous noise and transient noise made of short duration pulses (i.e. glitches) are of concern. One category of noise is seismic, acoustic and electromagnetic disturbances generated in the detector environment by its infrastructure machinery. For example, electro-mechanical devices such as air conditioners (serving the Buildings experimental clean area) and air compressors (serving vacuum valves), which contain fans and powerful engines that emit both continuous and transient noise. This transient noise is usually attributed to the switching on of a water chiller pump, which produces a fast inrush current of several Amps peak to peak.

The seismic, acoustic and electro-magnetic activity in each experimental building is constantly monitored by a number of fast sensors (sampling rate of 1kHz or more): seismometers, microphones, magnetometers, voltage probes, and current probes. In addition, the Infrastructure Machines Monitoring System (IMMS) consists of a number of slow probes (sampling rate of 1 Hz or less) monitoring the operating conditions of the machinery by measuring the temperature of the cooling/heating fluids of the air conditioning devices as well as measuring the pressure of air compressors. These signals, also known as “auxiliary” channels, are digitized by the Virgo Data Acquisition system, time-stamped with the GPS clock and made available for data-analysis together with the main ITF output (“h”) and a number of other ITF control signals.

Since gravitational wave detectors are susceptible to a large variety of interferences, a specific area of research known as DETCHAR has been established in order to identify and characterize noise [1]. Specialized monitors and software tools are created to study the detector noise and investigate on possible sources, eventually reducing their impact on the detector. Magnetic transients are a potentially relevant disturbance. External magnetic fields couple into the detector output signal (known as the “dark fringe” signal) via the magnetic actuators attached to the VIRGO suspended mirrors and used to keep the optics aligned. These glitches reduce the sensitivity of searches for GWs.

Within Virgo, the primary online software tool used to assist in the process of identifying glitches is *Omicron*. Omicron, a newer generation of Omega [3], which uses an algorithm primarily designed to identify gravitational wave, bursts, is rather useful in its applications to DETCHAR. Omicron processes data (both “h” and auxiliary channels) based on a specialized time-frequency “cluster finding” algorithm and outputs “triggers”, which give time, frequency, and signal to noise ratio (SNR) information about glitches in the data [7].

The work described in this paper analyzes Omicron triggers for a five-day period during the last Virgo Scientific Run VSR4, which took place between June 3rd and September 3rd 2011. This analysis aims to identify magnetic glitches in the h channel and provide clues to their origin. The process works by looking for statistically significant correlations between the Omicron triggers in h and a set of magnetic, voltage and current probe channels (hereafter “AUX” channels). The analysis algorithm is inspired by the Used Percentage Veto (UPV) analysis [4], which adds graphical tools for easing the identification of statistically significant data sub-sets (i.e. Regions of Interest – ROI). While the UPV is designed to develop vetoes, the uses for DETCHAR are only concerned with finding a source.

A follow-up analysis is then performed over these selected trigger sub-sets searching for time correlation with IMMS channels. Eventually we derive some information on the noise path and source. In the “Methods” section we describe the analysis steps, In the Results section we describe the follow-up analysis of selected ROIs. In Section 4 we discuss the results and future steps.

Methods

A *MatLab* code is created which reads Omicron triggers of the h and AUX channels and finds time coincidences between all channel pairs, thus selecting samples of “coincident” triggers. For each channel the signal to noise ratio (SNR) variable is considered, where SNR measures the “intensity” of

the glitch with respect to background noise, and its probability distribution is computed. For each channel pair, the code then computes and graphically compares the compound probability distribution of the coincident triggers with that of the full samples. Visually inspecting the graph, we then select SNR regions of coincident triggers that show a probability, which looks to be substantially above that of the uncorrelated triggers' background. We name these Regions of Interest (ROI). The ROI triggers are then plotted in time and compared to IMMS channels for investigating possible correlations with the operating cycle of infrastructure machinery, thus possibly identifying their origin.

In the following paragraphs details are given of the analysis: 1) Used Parameters, 2) Time coincidence, 3) SNR.vs.SNR graph, 4) ROI selection. In the Results section there is discussion of the follow-up analysis of selected ROIs.

Used Parameters

Omicron initially provides the channel triggers in a “.root”¹ format but for convenience are converted via a *MatLab* script into a C-structure variable and saved in “.mat” files. These structures contain the GPS time, SNR, Frequency and Time (with respect to the beginning of the five day run) information of a specified channel. Names and the corresponding output of the channels used in this analysis is provided in (Table I) and (Table II).

CHANNEL NAME	
V1: h_4096Hz	Calibrated Interferometer Output, Dark Fringe
V1: Em_IPSCB_50Hz	Voltage Probe on IPS cable in the Central Building
V1: Em_IPSMC_50Hz	Voltage Probe on IPS cable in the Mode Cleaner
V1: Em_IPSMC_CUR1	Current Probe on IPS cable in the Mode Cleaner Building
V1: Em_IPSNE_tmp	Voltage Probe on the IPS cable in the North End Building
V1: Em_IPSWE_tmp	Voltage Probe on the IPS Cable in the West End Building
V1: Em_MABDCE02	Magnetometer in the Central Building
V1: Em_MABDMC02	Magnetometer in the Mode Cleaner Building
V1: Em_MABDNE02	Magnetometer in the North End Building
V1: Em_MABDWE01	Magnetometer in the West End
V1: Em_UPSDET01_tmp	Voltage Probe on the UPS cable in the Central Building
V1: Em_UPSMC_CUR1	Current Probe on the UPS cable in the Mode Cleaner
V1: Em_UPSMC_50Hz	Voltage Probe on the UPS cable in the Mode Cleaner
V1: Em_UPSNE_tmp	Voltage Probe on the UPS cable in the North End
V1: Em_UPSWE_tmp	Voltage Probe on the UPS cable in the West End

(Table I) The list of analyzed channels. The “V1:” notation will not be carried on throughout the paper but is necessary to add when searching Data Display. These fast auxiliary channels are sampled at a rate of 1 kHz or more. It is also important to note that IPS stands for *Interrupted Power Supply* while UPS is *Uninterrupted Power Supply*, where both carry electric power throughout Virgo to different electromechanical devices.

CHANNEL NAME	
IMMS_TEMC51_OUTLCW	Temperature probe monitoring water coming out of Water Chiller (part of Air Conditioning system) near the Mode Cleaner
IMMS_TEMC51_INLCW	Temperature probe monitoring water coming in the Water Chiller (part of Air Conditioning system) near the Mode Cleaner
IMMS_TENE11_INLCW	Temperature probe monitoring water coming in the Water Chiller (part of Air Conditioning system) near the North End Building
IMMS_TENE11_INLWW	Temperature probe monitoring water coming in the Water Heater (part

¹ More information on .root files: <http://root.cern.ch/drupal/>

	of Air Conditioning system) near the North End Building
IMMS_TENE11_OUTLCW	Temperature probe monitoring water coming out of Water Chiller (part of Air Conditioning system) near the North End
IMMS_TENE11_OUTLWW	Temperature probe monitoring water coming out of the Water Heater (part of Air Conditioning system) near the North End Building
IMMS_TEWE11_INLCW	Temperature probe monitoring water coming in the Water Chiller (part of Air Conditioning system) near the West End Building
IMMS_TEWE11_INLWW	Temperature probe monitoring water coming in the Water Heater (part of Air Conditioning system) near the West End Building
IMMS_TEWE11_OUTLCW	Temperature probe monitoring water coming out of Water Chiller (part of Air Conditioning system) near the North End
IMMS_TEWE11_OUTLWW	Temperature probe monitoring water coming out of the Water Heater (part of Air Conditioning system) near the North End Building
IMMS_PRNE13_CA	Pressure probe monitoring the air compressor in the North End Building

(Table II) These *Infrastructure Machines Monitoring System* (IMMS) channels are responsible for the constant monitoring of the machinery incorporated into the infrastructure at Virgo. Also known as trend data, these channels are sampled at a rate of 1 Hz.

Time Coincidence

The premise behind a time coincidence is that if a glitch detected by a probe (i.e. a magnetometer) occurs at the same moment, or near the same moment (considering propagation time), as a glitch in the dark fringe channel it is most likely due to an environmental source and not a gravitational wave. The time coincidence performed for this analysis was done through a function in *MatLab*, which follows a time coincidence algorithm² with a threshold window of 0.1 seconds.

SNR vs. SNR plots

This section includes an example figure and explains the plots it contains in slight detail. Plots in **(Figure. 2)** shows the analysis of a channel pair: the probe monitoring electric current of the main IPS power cable in the Mode Cleaner Building (also named “Channel X”) and one Magnetometer in the Mode Cleaner Building (also named “Channel Y”). In the following we consider the data sets: (1) the SNR of all channel X triggers; (2) the SNR of all channel Y triggers; (3) the SNR of channel X triggers which are coincident with channel Y; (4) the SNR of channel Y triggers which are coincident with channel X.

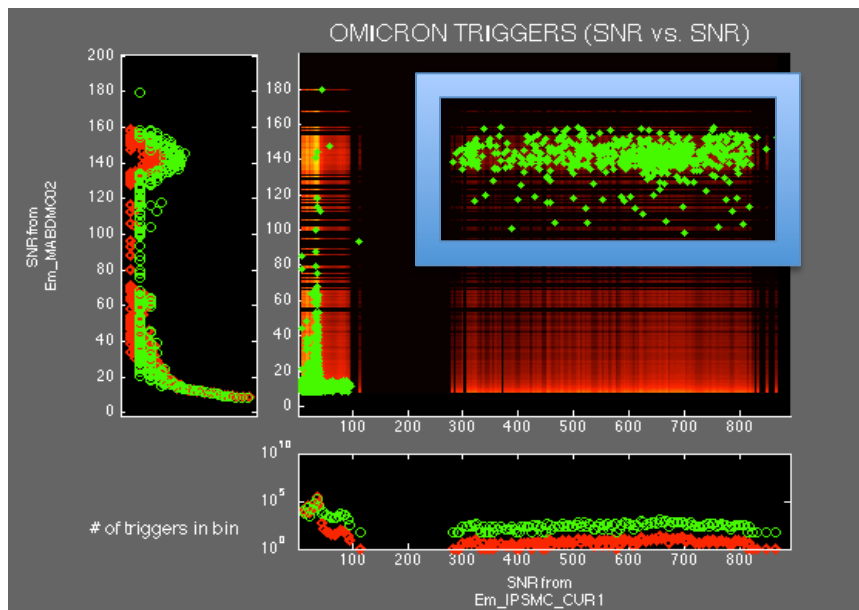


(Figure 2) This figure is displaying 3 subplots: two along the axes of the central plot and the SNR vs. SNR plot. This particular plot is showing the coincident triggers between the Ammeter in the Central Building (*Em_IPSMC_CUR1*) and a Magnetometer in the Mode Cleaner (*Em_MABDMC02*). The blue box is an established ROI (discussed below)

The graph in (**Figure 2**) shows multiple subplots. The two plots along the x and y axes are histograms displaying the probability distribution of a specified SNR data set in a channel. The height of each dot on the histogram reflects the likeliness of finding a trigger located at a specific bin (which characterizes an SNR interval varying on the size of the bin) for a specific set of data whether it is “all” triggers (red) or coincident (green) triggers. More precisely, the red histograms reflect the likeliness of locating any trigger in a bin “i”:

$$(Eq. 1) \quad \text{Height of Red dot} = \text{Number of triggers in bin}_i = \text{Probability}_{\text{Bin}_i}$$

The green dot histogram reflects the probability of finding a coincident trigger in a specific bin (normalized to the total number of triggers in the channel):

$$(Eq. 2) \quad \text{Height of Green dot} = \frac{\text{Number of coincident triggers in bin}_i}{\sum \text{Coincident triggers}} * \sum \text{All the triggers} = \text{Probability}_{\text{Bin}_i}$$

By design the histograms are normalized to the total number of triggers in the channel so that this holds true:

$$(Eq. 3) \quad \sum \text{All Triggers in Channel} = \sum \text{Heights of Green Dots} = \sum \text{Heights of Red Dots}$$

In the central plot, a hot color map background displays a two dimensional probability distribution that reflects the likeliness of a finding a trigger located at pixel (or bin intersection) by how “hot” it is. Given a pixel in the SNR vs. SNR plane identified by the bin indexes pair numbered (i,j), two dimensional probability is computed as the product of the single probability of X and Y channel (as defined in Eq.1 and Eq. 2):

$$(Eq. 4) \quad \text{Chance of finding trigger at a Pixel} = \text{Probability}_{\text{Bin}_i} * \text{Probability}_{\text{Bin}_j}$$

$$(Eq. 5) \quad \text{Probability}_{\text{Bin}_x} = \frac{\sum \text{Triggers from Channel } x \text{ in Bin}_i}{\sum \text{All Triggers in Channel } x}$$

$$(Eq. 6) \quad \text{Probability}_{\text{Bin}_y} = \frac{\sum \text{Triggers from Channel } y \text{ in Bin}_j}{\sum \text{All Triggers in Channel } y}$$

Where Channel x and Channel y are the channels at the noted axes.

In the central plot, overlapped to the hot color map, is the scatter plot of the coincident dataset (green dots).

Region of Interest

ROI are established when interesting data, such as trigger clusters, are present. When observing a trigger cluster between two channels, for example the blue box in (**Figure 2**), it indicates that either one channel is coupling into the other, or both share a common source. In the case of (**Figure 2**) the ROI indicates the latter. When plotting an auxiliary channel against the Interferometer output channel it usually indicates the former; therefore the incentive behind these specific plots is the identification of a coupling source. A *MatLab* script was written in order to isolate and store the information of the ROI data subsets (trigger clusters) onto the *MatLab* workspace. The trigger information then allows us to plot the ROI triggers in time, which may show correlation to the periodic behavior of the infrastructure machinery used at Virgo.

As a sanity check, a fake 10-second offset is added to the time vector of one of the two channels. The presence or absence of green triggers gave indication of fake or real coincidence, respectively.

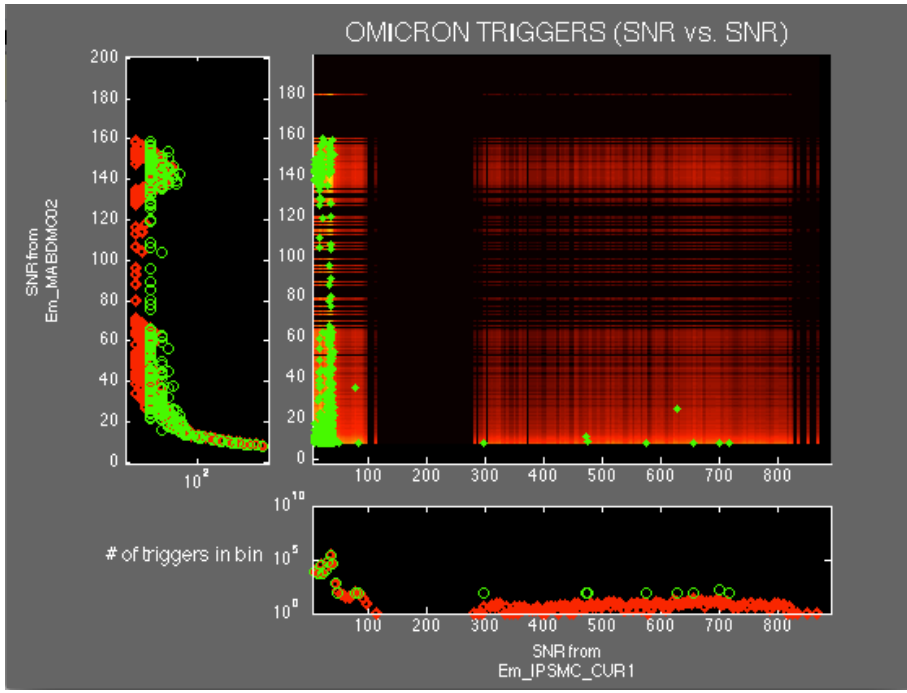


(Figure 3) This figure is the same plot as **(Figure 2)** with the fake ten-second offset added

A question has been posed in regards to the usage of SNR vs. SNR plots as opposed to Frequency vs. Frequency plots. The nature of how far or near a source is to the Dark Fringe can be considerably noticed by the glitch signal to noise ratio while glitch frequency, for electromechanical sources, remains constant at all distances therefore multiple sources with the same frequency cannot be differentiated. For frequency glitches it is expected that there be a linear trend through the origin, which characterizes freq_x = freq_y. Only in the case of up conversion there will be some visual clustering. In this case, such a phenomena is not observed. Also, since the frequency plots are expressed in discreet values plotting overlap is more likely to occur and is harder to establish a proper ROI (i.e. For electrical glitches this occurs at the 50 Hz frequency). Therefore, it can be proven, that more information about a particular source tends to be stored in the time-coincident, signal to noise ratio pairs. A frequency plot with the same two channels found in **(Figure 2)** can be found in **(Figure 4)**.

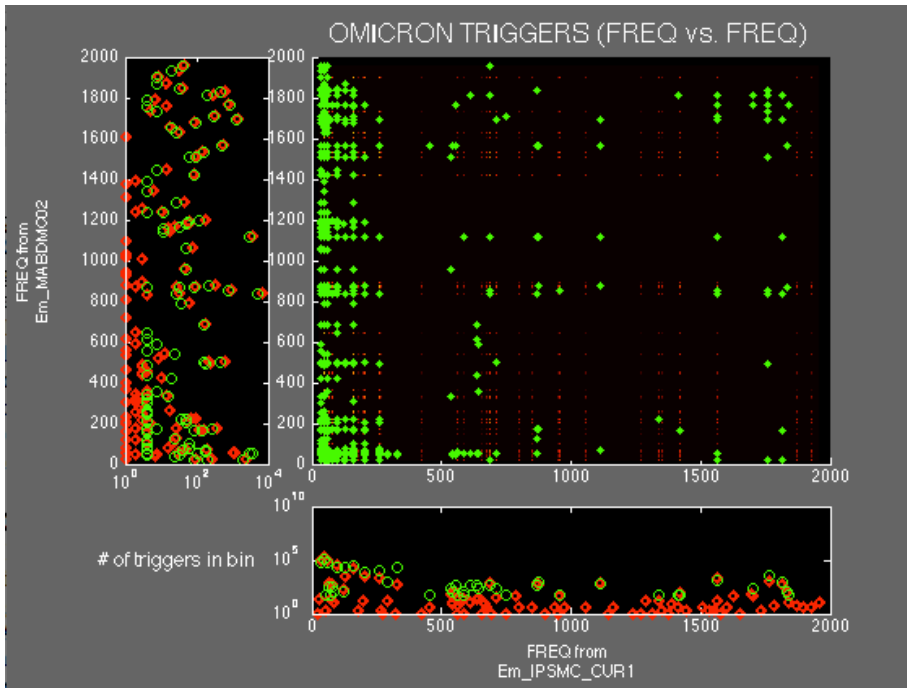


(Figure 4) In the given frequency plot, information about a particular source is more ambiguous. The isolation of the clusters in the SNR plots is what gives them a major advantage in identifying a particular noise source. The histogram technique of examining the data also offers (in this case) little to no information on how to properly extract the data.

RESULTS

Local to the Mode Cleaner Building (MC), there appears to be much evidence supporting magnetic activity, which is strong enough to show continuous coupling to the DF. There was also magnetic activity detected in the Terminal buildings, which displayed little but present coupling to the DF.

A hypothesis was made long before this investigation that the Virgo Air Conditioning systems, which function on a water chillers as well as a water heaters, might be responsible for magnetic activity in the DF [1]. The water chiller specifically has been known to periodically switch on inducing a strong inrush current and producing a brief magnetic disturbance. This was found originally in the analysis of VSR2 data [1]. Afterwards Virgo was updated to Virgo+ where it was found and measured that the magnetic disturbance was reduced by a factor of five [5].

The following is the first, thorough search of possible magnetic glitches coupling to Virgo+ through VSR4 data as well as a follow-up investigation of their sources

No.	Channel Pairs (x vs. y)	ROI (x-limits) (SNR)	ROI (y-limits) (SNR)	Correlation to:
1	Em_MABDMC02 vs. h_4096Hz	100 - 160	7 - 15	MC Water Chiller
2	Em_IPSMC_CUR1 vs. h_4096Hz	290 - 900	7 - 15	MC Water Chiller
3	Em_IPSMC_50Hz vs. h_4096Hz	100 - 260	7 - 15	MC Water Chiller
4	EM_MABDCE02 vs. h_4096Hz	10 - 65	7 - 15	MC Water Chiller
5	Em_MABDNE02 vs. h_4096Hz	170 - 210	7 - 10	MC Water Chiller
6	Em_IPSNE_tmp vs. Em_MABDNE02	40 - 360	130 - 210	MC Water Chiller
7		60 - 180	22 - 38	NE Air Compressor
8	Em_MABDWE01 vs. h_4096Hz	45 - 80	7 - 20	WE Water Chiller
9	Em_IPSWE_tmp vs. Em_MABDWE01	80 - 420	45 - 90	WE Water Chiller
10	Em_IPSWE_tmp vs. Em_IPSNE_tmp	25 - 150	25 - 150	Not Found
11		150 - 400	10 - 30	WE Water Chiller
12		10-30	150 - 400	NE Water Chiller
13	Em_IPSNE_tmp vs. Em_IPSCB_50Hz	20 - 130	20 - 80	Not Found
14	Em_IPSWE_tmp vs. Em_IPSCB_50Hz	20 - 130	20 - 80	Not Found

(Table III) This is a list of Channel pair, their boxed limits of the ROI taken, and the final correlations of these data subsets to operating machinery (when found).

Mode Cleaner

The magnetometer in the Mode Cleaner building was by far the strongest contender in showing the largest production of coincident triggers with the DF data³. Evidence of this can be seen in **(Figure 5)**, while **(Figure 6)** shows a ROI between the Interferometer Output Channel and a current probe in the MC. The ROIs found **(Figure 5)** and **(Figure 6)** will show to share a common source.

³ For these particular 5 days of VSR4

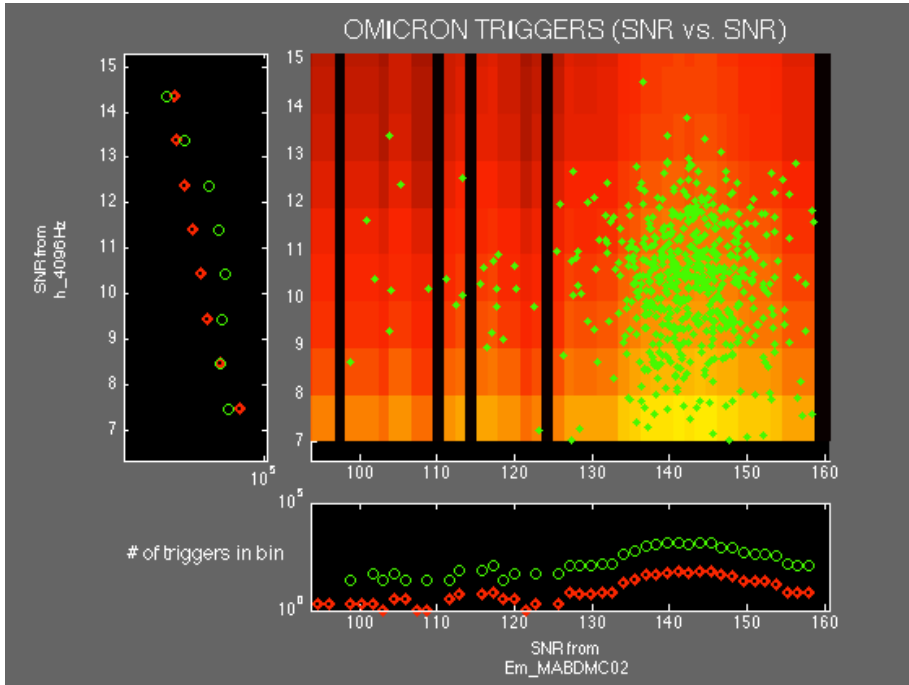


(Figure 5) Shows a region of interest (ROI) that was found in the SNR vs. SNR plot of the triggers from the Magnetometer in the Mode Cleaner (*Em_MABDMC02*) vs. the Interferometer Output channel (*h_4096Hz*). It is important to note that the SNR values for the Magnetometer span from 100 to 160, and for the Dark Fringe channel they span from 7 to 15.

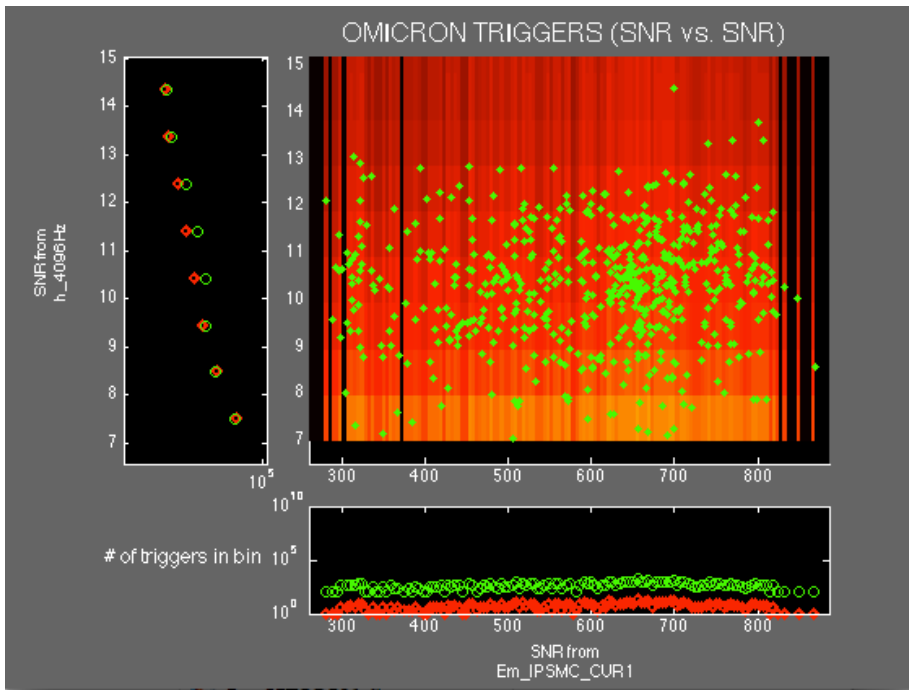


(Figure 6) This is a plot of a Current Probe in the Mode Cleaner (*Em_IPSMC_CUR1*) vs. the Dark Fringe Channel (*h_4096Hz*). Taking into account the SNR interval of the Dark Fringe triggers (SNR 7-15) from **(Figure 2)**, it is safe to say that these triggers are caused by an on-site electromagnetic phenomenon.

Triggers in the selected ROIs were then plotted in time with the IMMS channels monitoring the temperature of the water in and out of the MC Chiller. As can be seen in **(Figure 7)** every 10 minutes, the water heats up to some relatively warm temperature thereby prompting the chiller to switch on, which will reflect a quick and dramatic decrease in temperature. It is evident from **(Figure 7)** that selected glitches are synchronized with chiller switches on.

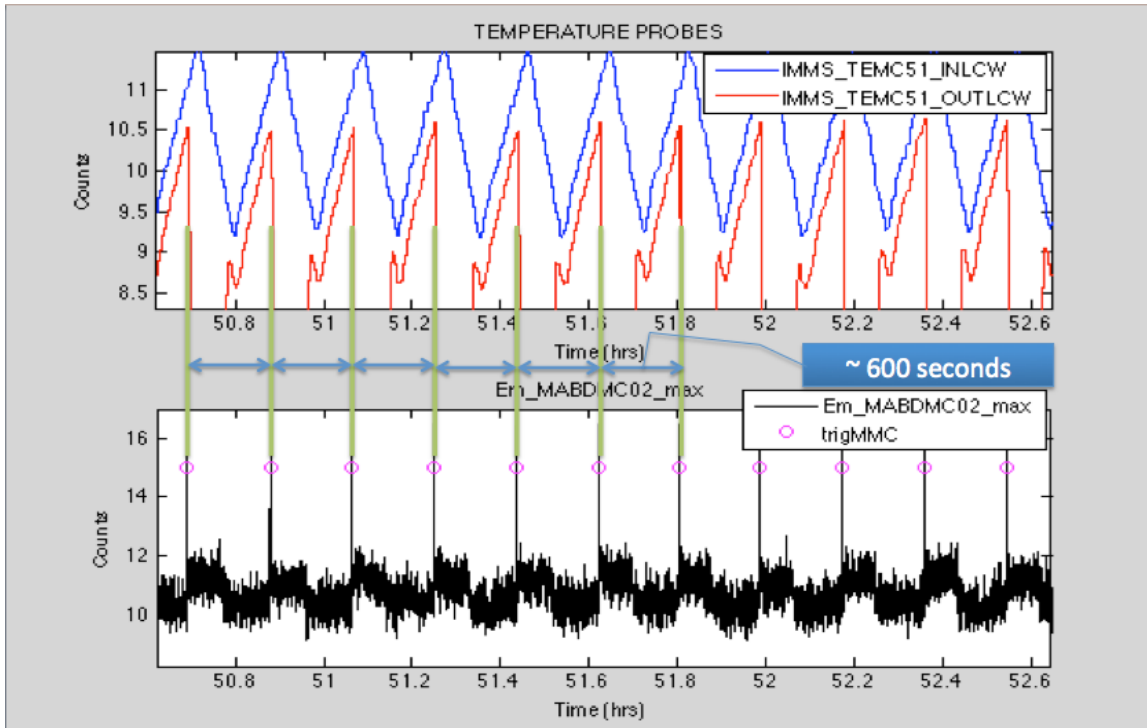


(Figure 7) The top subplot shows the behavior of the temperature water in time going out of the chiller (IMMS_TEMC51_OUTLCW) and going into the chiller (IMMS_TEMC51_INLCW). The Vertical scale value is Temperature in Units of Degrees Celsius. The bottom subplot shows the corresponding magnetometer maxima (EM_MABDMC02_max) and the matching triggers (trigMMC) taken from the ROI in **(Figure 5)**. The vertical scale is showing arbitrary units. The purpose of this plot was intended to display the time information of these triggers. After assigning a value of one to the triggers, an arbitrary factor of fifteen was multiplied to the set for easy visualization.

Triggers from **(Figure 5)** and **(Figure 6)** as well as triggers from the MC Voltage Probe and magnetic probe in the Central Building (Table III, rows 1-4) were plotted in time with the magnetometer triggers in the Dark Fringe in order to verify the synchronicity.

Finding the same “MC chiller “glitches present in all of these probes gives hints apropos to the noise path into the dark fringe. A suggested noise path states that the MC chiller switches on, produces an extra current running through the power cables as measured by the current probe (EM_IPSMC_CURR), the extra current generates a magnetic pulse seen by the local magnetometer (Em_MABDMC02) as well as a voltage drop in the MC building and CB buildings (Em_IPSMC_50Hz and Em_IPSCB_50Hz probes)⁴. The voltage drop in the CB building results in a generated magnetic field pulse (seen by Em_MABDCE02), which eventually couple to the sensitive mirrors. This is the same path hypothesized and tested for the Magnetic noise from the MC electric heater to the GW channel during VSR1 [6].

Terminal Buildings (North End and West End)

The trigger contributions found in the terminal buildings cannot compare to the activity to the Mode Cleaner but their existence in the Dark Fringe deems it necessary to investigate. In these sets of data it was more difficult to choose an obvious ROI since data points were so few. The West End showed only a handful of triggers which might be attributed to the infrastructure machinery while the North End only showed two (see **(Figure 8)**).

⁴ Note: This should not happen for an ideal voltage source, therefore it seems as if the MC and CB IPS do not behave as ideal sources.

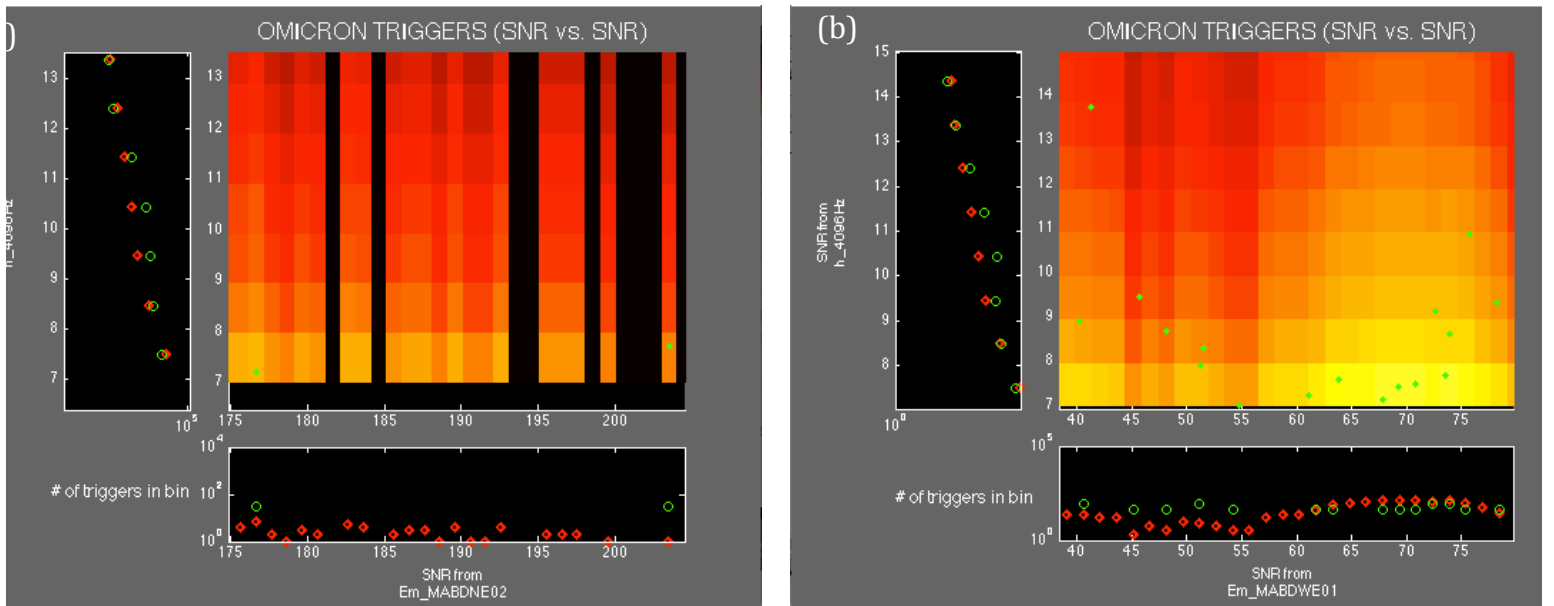


(Figure 8) (a) Zoomed in ROI for the Magnetometer in the North End and the Interferometer output channel. Only two triggers appear to be present. (b) Zoomed in ROI for the Magnetometer in the West End and the Interferometer output channel.

This set of data underwent the same investigations as the Mode Cleaner data. After this was done, the periodicity check (see **(Figure 9)**) revealed that the adjacent water chillers located at these buildings are responsible for these triggers.

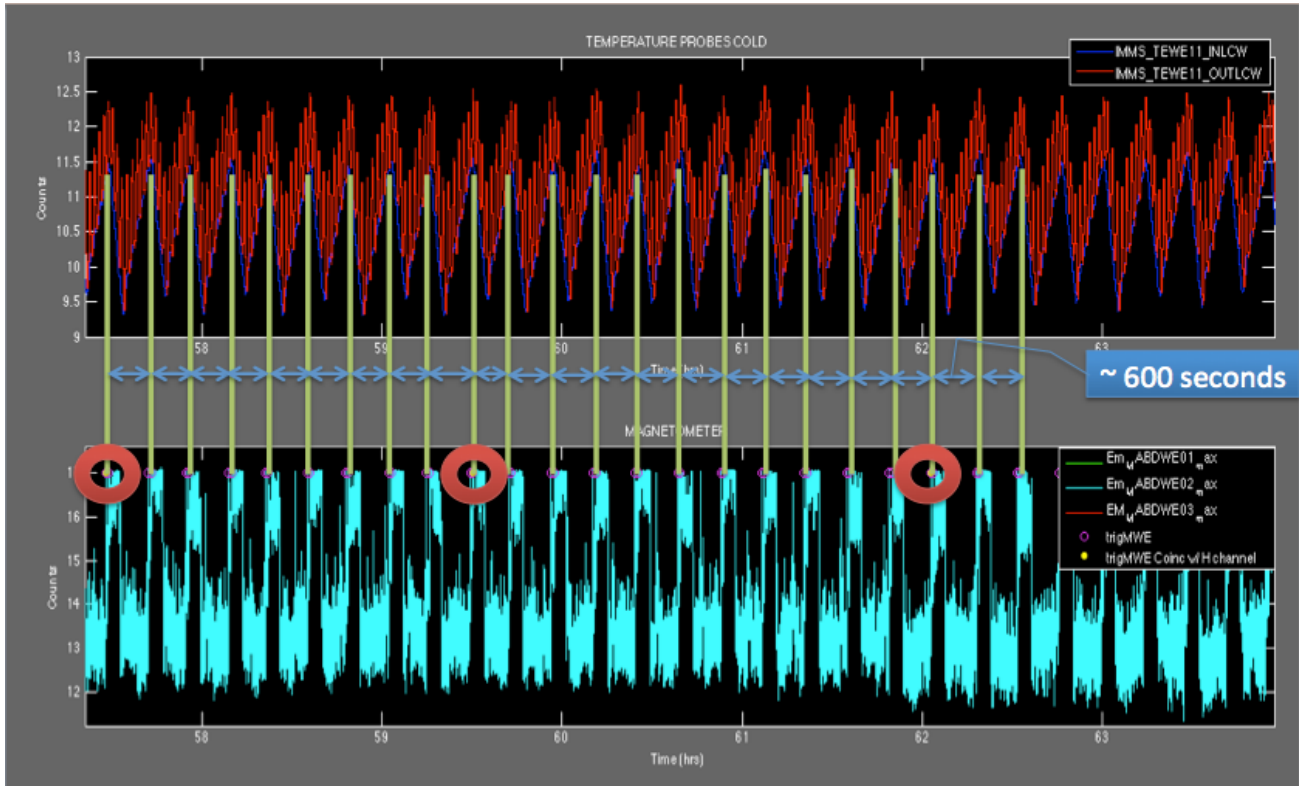


(Figure 9) This is a periodicity check for the magnetometer in the West End Building. The Blue spikes are the Magnetometer maxima, the magenta holes are coincident triggers found between a voltage probe in the West End (*Em_UPSWE_tmp*) and the magnetometer in the west end (*Em_MABDW02*). The yellow dot triggers (in the red circles) that correspond to magnetometer spikes show a correlation to the temperature probes. This confirms that the chiller indeed is responsible for the triggers in **(Figure 5)(b)**. The average time interval in between these pairs of triggers is about 10 minutes.

Other Magnetic Sources

This final section is intended not to show any activity in the Dark Fringe but to note for future reference the existence of triggers due to the air compressor. This magnetic activity due to this air compressor device is only noticed in the North End building and the cluster of triggers that gave evidence of this behavior was found as a ROI when examining the SNR vs. SNR plot of two auxiliary channels, specifically a Magnetometer (Em_MABDNE02) with a Voltage Probe in the North End (Em_IPSNE_tmp).

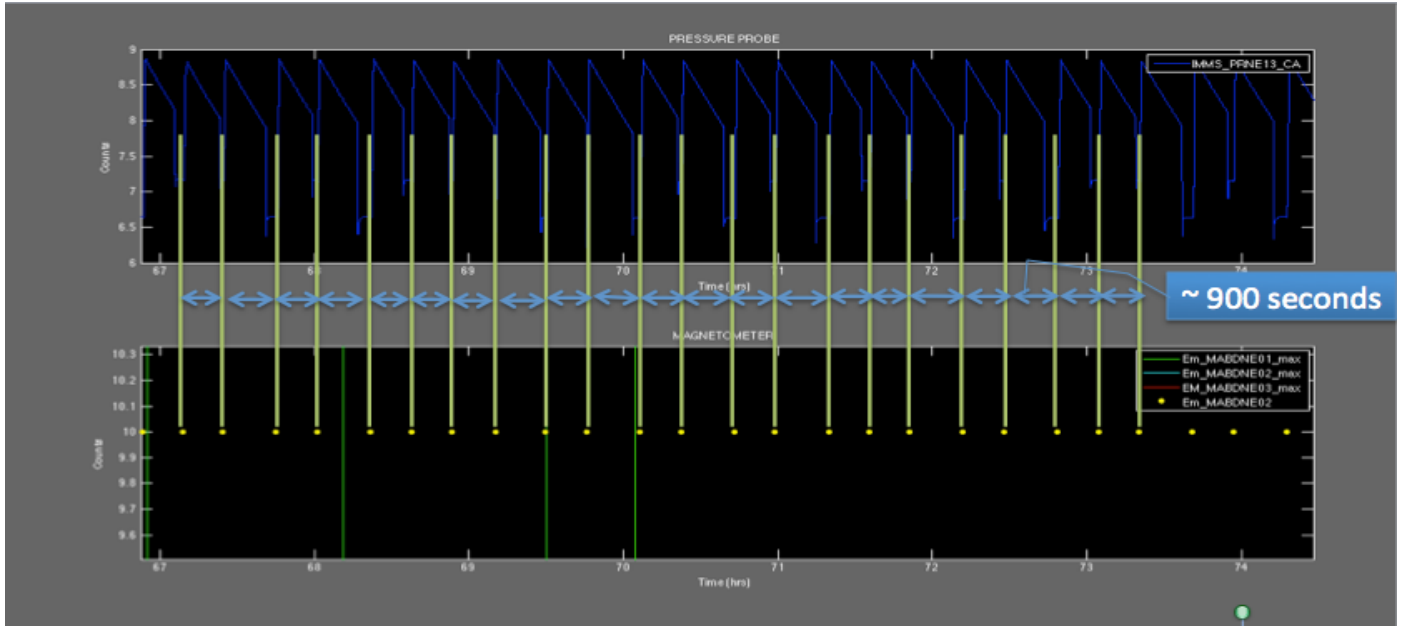


(Figure 10) This plot shows the time coincidence between the yellow magnetometer triggers (bottom plot) from a plot of two auxiliary probes against one another (Voltage probe in the North End vs. the Magnetometer in the North End) and the periodic switching of the pressure probe (IMMS_PRNE13CA). The average time interval in between these triggers is about 900 seconds.

Global Noise

An interesting feature given by this analysis is a correlation of glitches between the Central Building, North Building and West Building Voltage Probes. An example of this, between the North End and West End, can be seen in **(Figure 11)**. The relationship between these three channels is suggested by the regions of interest in Table III, No. 10-12)

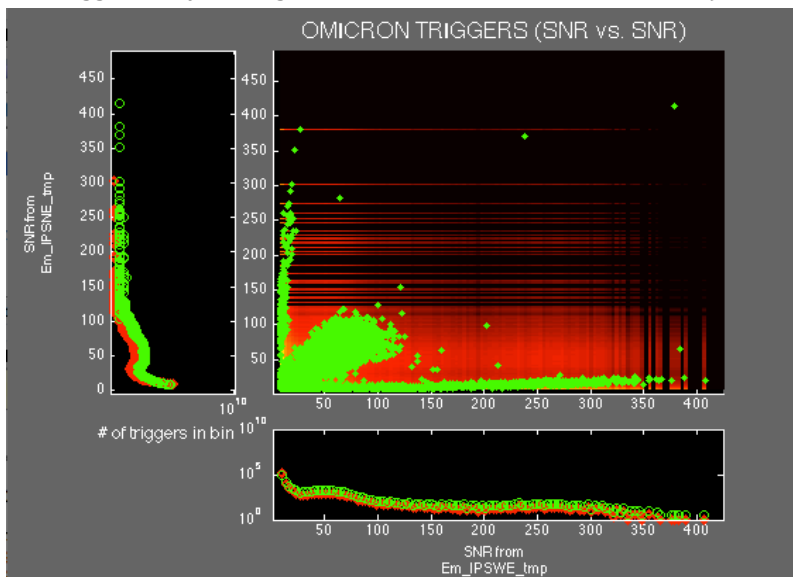


(Figure 11) Voltage Probe in the West End Building (Em_IPSWE_tmp) vs. Voltage Probe in the North End Building (Em_IPSNE_tmp).

When the fake ten-second offset was added the 3 clusters disappeared suggesting real coincidence, but in order to take extra precautions, the time differences (dt) between an event in two channels were plotted on a histogram as shown in **(Figure 11)**. The majority of time differences are clustered about zero indicating that they are real coincidences. The time difference check along with the original diagnostics suggests that the central cluster is real coincidence but information in regards to origin is yet to be found. A hypothesis is that this cluster is related to a disturbance travelling through the power lines.

Sources were assigned to the side clusters along the x and y axes, which are noted in **(Table III)** **No. 11 and 12.**

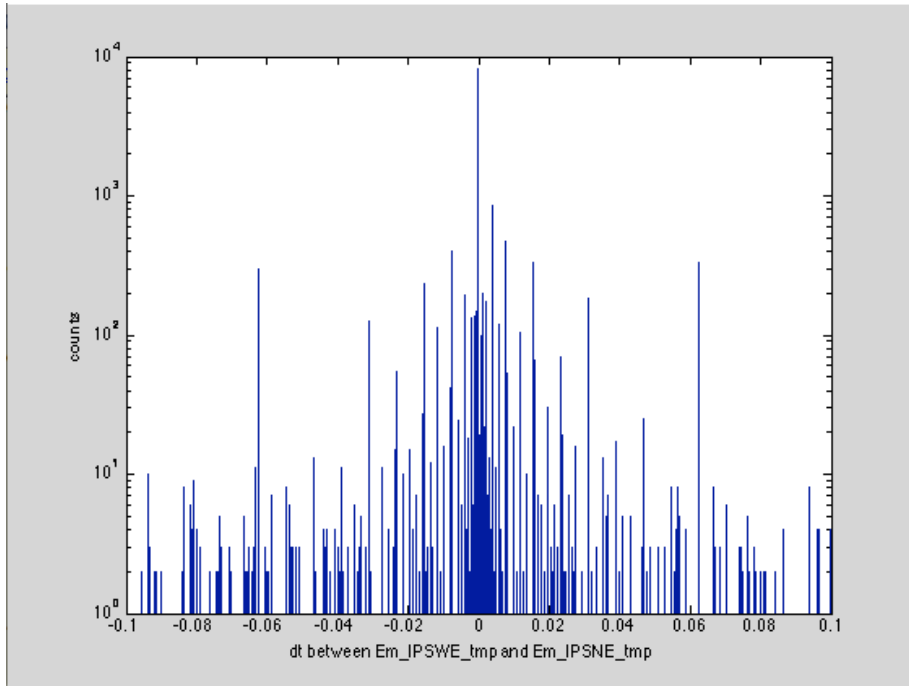


(Figure 12) A histogram documenting where the time differences (produced by the time-coincidence) for the central cluster in **(Figure 11)** on an interval from 0 to the .1-second threshold. It seems apparent that the majority lies near zero; therefore the data appears to be trustworthy.

Conclusion

Magnetic noise sources that pervade the Virgo environment have given enough information, through this analysis, to verify hypotheses as well as initiate a discussion on mitigation methods. There have already been discussions on how to mitigate the noise produced by these cables (i.e. the proposition of a twisted wire method) [7], but if mitigation methods are not implemented, there will be no other option but to veto these transients and as a consequence increase dead time, adding more constraints to science run time.

References

- [1] Asi J., et al., The characterization of Virgo Data and its impact on gravitational-wave searches, *Class. Quantum Grav.* 29 (2012) 155002
- [2] Braccini S., et al. A Measurement of the seismic attenuation performance of the VIRGO Superattenuator. *Astroparticle Physics* 23 (2005) 557-565
- [3] Chatterji S., et al., Multiresolution techniques for the detection of gravitational wave bursts *Class. Quantum Grav.* 21 (2004) S1809-S1818
- [4] Isogai T., Used Percentage Veto for LIGO and Virgo Binary Inspiral Searches *Journal of Physics: Conference Series* 243 (2010) 012005
- [5] Swinkels B., et al., Magnetic injection from the near-field, monolithic edition, *Virgo Logbook*, 28260, https://tds.ego-gw.it/itf/osl_virgo/index.php?callRep=28260
- [6] Swinkels B., et al., MC building powered by generator #2, *Virgo Logbook*, 26758, https://tds.ego-gw.it/itf/osl_virgo/index.php?callRep=26758
- [7] Robinet F., Omicron: a tool for detector characterization, Virgo TDS, VIR-0296A-12, <https://tds.ego-gw.it/ql/?c=9364>

ACKNOWLEDGEMENTS

This project was funded by: the National Science Foundation through the University of Florida's Gravitational Wave physics IREU program as well as the Istituto Nazionale di Fisica Nucleare (INFN), and the University of Pisa. The authors gratefully acknowledge the support of the United States National Science Foundation for the construction and operation of the LIGO Laboratory, the Science and Technology Facilities Council of the United Kingdom, the Max-Planck-Society, and the State of Niedersachsen/Germany for support of the construction and operation of the GEO600 detector, and the Italian INFN and the French Centre National de la Recherche Scientifique for the construction and operation of the Virgo detector. The authors also gratefully acknowledge the support of the research by these agencies and by the Australian Research Council, the International Science Linkages program of the Commonwealth of Australia, the Council of Scientific and Industrial Research of India, the Istituto Nazionale di Fisica Nucleare of Italy, the Spanish Ministerio de Economía y Competitividad, the Conselleria d'Economia Hisenda i Innovació of the Govern de les Illes Balears, the Foundation for Fundamental Research on Matter supported by the Netherlands Organisation for Scientific Research, the Polish Ministry of Science and Higher Education, the FOCUS Programme of Foundation for Polish Science, the Royal Society, the Scottish Funding Council, the Scottish Universities Physics Alliance, The National Aeronautics and Space Administration, the Carnegie Trust, the Leverhulme Trust, the David and Lucile Packard Foundation, the Research Corporation, and the Alfred P Sloan Foundation.